

Chapter 9

H6: Steady Flow through a Gate

Contents

9.1	Problem Specification	9-1
9.2	Initial Transients	9-3
9.3	Numerical Filtering	9-4
9.4	Contra Costa Water District	9-5
9.5	Department of Water Resources	9-12
9.6	Resource Management Associates	9-17
	REFERENCES	9-17

9.1 Problem Specification

H6 Steady flow through a channel gate

Focus gate and boundary transients, network connectivity.

Channel bed is horizontal from upstream point A to downstream point D (see Figure 9.1). The trapezoidal channel bed width B is 50 ft. At A, $x_A = 0$ ft and $Z_A = -20.0$ ft. At D, $x_D = 50,000$ ft and $Z_D = -20.00$ ft. Channel friction factor is constant at Darcy-Weisbach $f = 0.03$ or Manning $n = 0.02$.

An underflow gate is located at $x_B = x_C = +20,000$ ft, with point B on the upstream side, and point C on the downstream side. At $t = 0$ s, the gate is fully open, and remains fully open throughout.

The hydrodynamic initial conditions at $t = 0$ s are quiescence:

$$\eta(x, 0) = 0 \quad \text{and} \quad Q(x, 0) = 0 \tag{9.1.1}$$

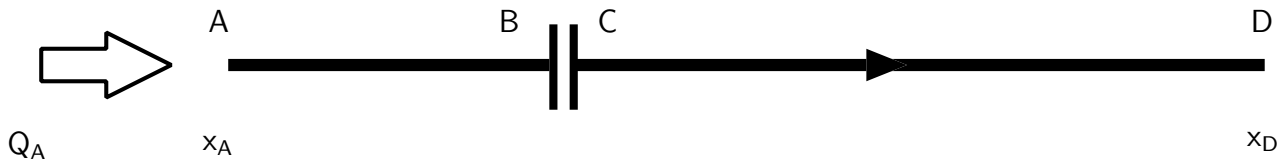


Figure 9.1: Definition sketch for Problem H6.

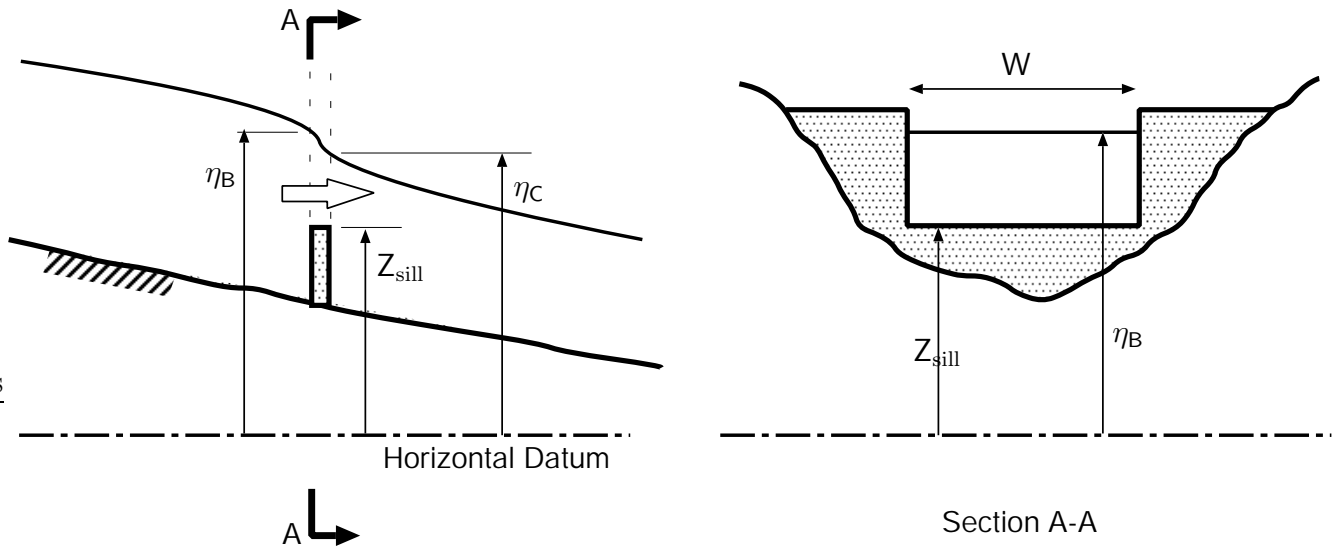


Figure 9.2: Longitudinal Profile and Cross-Section at Gate

The gate (see Figure 9.2) operates with steady throughflow following

$$Q = C_G A_G (2g\Delta\eta)^{1/2} \quad (9.1.2)$$

The gate discharge coefficient C_G is 0.5. The water surface elevation difference across the gate is $\Delta\eta = |\eta_B - \eta_C|$, the flow being in the direction of falling elevation. The gate flow area is

$$A_G = \begin{cases} W [\max(\eta_B, \eta_C) - Z_{\text{sill}}] & \text{for } \max(\eta_B, \eta_C) > Z_{\text{sill}} \\ 0 & \text{for } \max(\eta_B, \eta_C) \leq Z_{\text{sill}} \end{cases} \quad (9.1.3)$$

where $W = 40$ ft is the uniform gate width, and $Z_{\text{sill}} = -15$ ft is the elevation of the sill.

Open boundary conditions are fixed at

$$Q_A(t) = +20,000 \text{ ft}^3/\text{s} \quad \text{and} \quad \eta_D(t) = +0 \text{ ft} \quad \text{for all } t > 0 \quad (9.1.4)$$

Use a fixed computational space step $\Delta x = 500$ ft and a fixed computational time step $\Delta t = 30$ s.

Compute and write to file in the STANDARD FORMAT the initial conditions at $t = 0$ and the model predictions for every 90 s (3 time steps) for 2.5 hours.

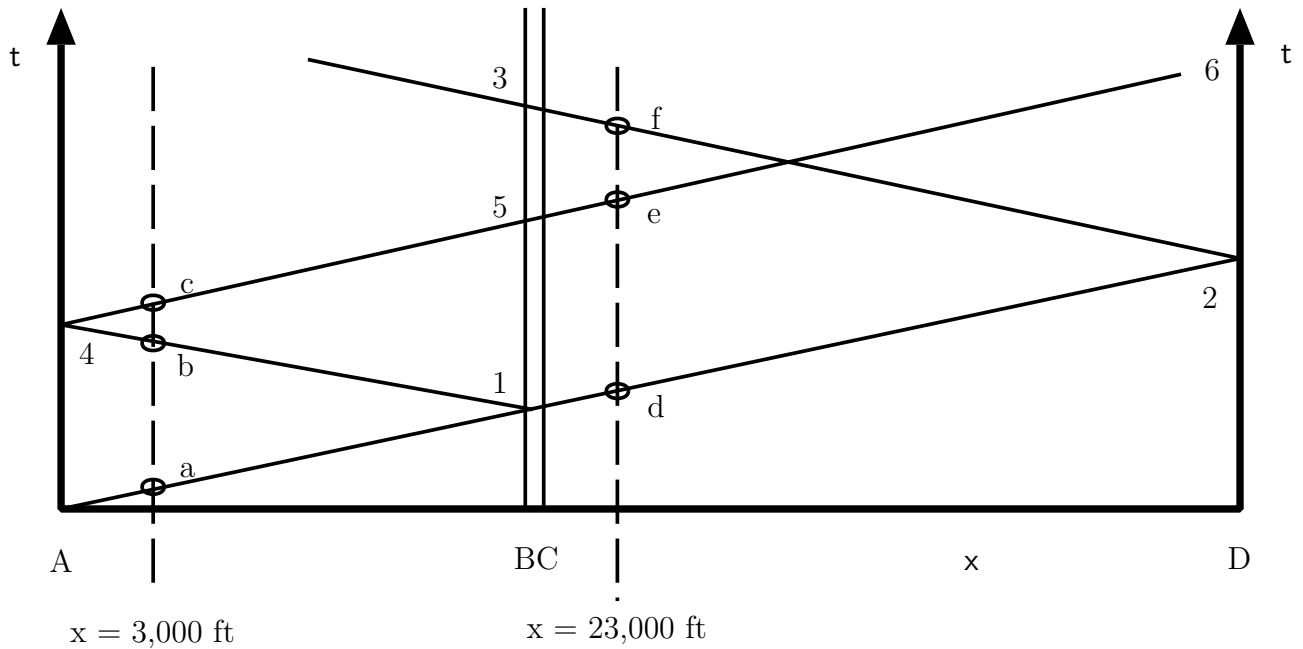


Figure 9.3: Characteristic Paths for Problem H6

9.2 Initial Transients

Channel gates have a hydrodynamically-significant role in the Bay-Delta circulation. Their objective is flow control. The hydraulics are well known (Equation 9.1.2), but are based on a steady flow argument and require an empirical coefficient C_G .

Initial transients are expected from two sources,

1. at A at $t = 0$ by the sudden change from the $Q = 0$ initial conditions to the $Q = +20,000$ ft^3/s boundary condition, and
2. at the gate BC by forcing the Equation 9.1.2 relationship between η and Q .

Equation 9.1.2 is empirical and steady. Flow in the neighborhood of the gate may be rapidly-varied in both space and time, and the gate condition may conflict with the gradually-varied conservation Equations 2.4.1 and 2.4.2. Even in the steady state, Equations 2.4.1 and 2.4.2 do not reduce to Equation 9.1.2.

There is an anecdotal record of difficulties with gates in estuarine channel models, though little detail appears in the published literature.

The sudden changes initiated at A and at BC, and the boundary reflections can be followed on the characteristic paths diagram, Figure 9.3. The initial disturbance propagates along path A123 from the upstream boundary, through the gate at 1 to the downstream boundary at 2, where it is reflected back through the gate at 3. Path 1456 is the initial reflection from the gate, re-reflection from the upstream boundary and propagation through the gate at 5 toward the downstream

boundary at 6. The initial disturbance is a step change at $x = 0$, so that all these disturbances are also step changes. Mass and momentum balances will be investigated at $x = 3,000$ ft and $23,000$ ft, marked as dashed lines. Disturbance intersections should be identifiable at points a through f.

Table 9.1 has been prepared as a aide in interpretation of the subsequent mass and momentum balances. It lists the travel distances along these characteristic paths to points a through f, and the time to reach these points. It has been assumed that the propagation speed along these paths

	a	b	c	d	e	f
x ft	3,000	37,000	43,000	23,000	63,000	77,000
t s	142	1752	2036	1089	2984	3647

Table 9.1: Distances and Times along Characteristic Paths

is approximately $\sqrt{gA_0/b_0} = 21.1$ ft/s throughout, where A_0 is the initial cross-section area and b_0 is the initial surface width.

9.3 Numerical Filtering

Significant free mode responses are a natural part of the present problem. These are inevitably short wave length modes, and confusingly suggestive of numerical instability. Though perhaps visually embarrassing, these free mode responses are not an indication of a numerical deficiency. They are the expected physical response to the forcing at A and the gate at BC.

The initial transients at A require particular attention. The transients are initiated by the rapid introduction of an inflow at A. In a theoretical linear approximation (Bode and Sobey 1984), this rapid change is communicated as an eigenmode expansion of the form

$$\begin{aligned}\tilde{\eta}(x, t) &= \exp(-\lambda t/2) \sum_{n=0}^{\infty} (A_n \cos \omega_n t + B_n \sin \omega_n t) \sin \beta_n x \\ \tilde{Q}(x, t) &= b_0 \exp(-\lambda t/2) \sum_{n=0}^{\infty} [(-\lambda A_n/2 + \omega_n B_n) \cos \omega_n t - (\omega_n A_n + \lambda B_n) \sin \omega_n t] \frac{\cos \beta_n x}{\beta_n}\end{aligned}\tag{9.3.1}$$

where $n = 0, 1, 2, \dots$ and the free mode wave numbers and frequencies are

$$\beta_n = \left(n + \frac{1}{2}\right) \frac{\pi}{L}, \quad \omega_n = C_0 \left[1 - \left(\frac{\lambda}{2C_0\beta_n}\right)^2\right]^{1/2} \beta_n\tag{9.3.2}$$

The A_n and B_n are listed in the appendix of Bode and Sobey (1984); these details are unnecessary here. λ is the linear friction coefficient and C_0 is the linearized phase speed. The leading wave number modes $\beta_n = 2\pi/L_n$ would correspond to wave lengths $L_n = 80,000$ ft, $26,667$ ft, $16,000$ ft, \dots . As this eigenmode expansion must follow the rapid initial change in Q , it must be dominated

by the higher modes (large n) for which the wave length is very short. But the discrete spatial resolution cannot resolve wave numbers beyond the Nyquist limit $\beta_N = \pi/\Delta x$ (Båth 1974). Longer wave numbers (shorter wave lengths) are aliased or folded about the Nyquist limit to shorter wave numbers (longer wave lengths). The resulting numerical response has a concentration of wave numbers just below the Nyquist limit, at wave length $L_N = 2\pi/\beta_N = 2\Delta x$. This aliased response, sometimes referred to a “ $2\Delta x$ ” modes, is expected in the initial Q evolution from A. Reducing the space step will change the apparent wave length of the aliased modes, but not eliminate them. As these are free modes, albeit aliased, they will be decayed by friction, as suggested by Equation 9.3.1. The appearance of these aliased free modes in the initial Q response is both natural and expected. It is natural because of the step change in the Q boundary condition at A. It is expected because to the finite spatial resolution, Δx , of the numerical representation.

This problem has two potential sources of local short wave length disturbances. Such disturbances draw immediate visual attention. They will not be observed in the real world, only in a numerical representation such as this. They are a direct and understandable consequence of efforts to represent “sub-grid scale” processes¹ in a discrete numerical model. They are expected. They are not an indication of some deficiency in a numerical model, but rather compelling evidence that the numerical model has been both well formulated and carefully coded.

But the very suggestion of some code deficiency leaves this problem very vulnerable to the “smooth is beautiful” disease. The wave lengths of free modes are often relatively short, and might be removed by low-pass filtering. But excessive filtering is a most undesirable feature of any numerical code that seeks physical integrity. In a classical contribution to the numerical modeling literature, Gresho and Lee (1981) warn

Don’t suppress the wiggles - they’re telling you something!

The message is clear and compelling. The **wiggles** have a crucial role to play, as indicators of potential problems. Filter code is not discriminating. It will remove physically appropriate responses along with numerical inconveniences.

Short wave length response might be suppressed by either

1. natural filtering by the adopted numerical algorithm, or
2. specific filter code to suppress gate transients

The former is not a physically desirable property of a numerical algorithm. The latter raises concerns about the wider impact of the gate filter.

9.4 Contra Costa Water District

Figure 9.4 shows the CCW-predicted η and Q evolution toward the steady state. This is a visually impressive result. The characteristic paths are shown very clearly, in particular the initial disturbance propagating from the upstream boundary, the reflection of this disturbance from the

¹Step change in Q boundary condition at A, and local rapidly-varied flow in neighborhood of gate.

gate (in the η plot) and from the downstream boundary (in the Q plot), the initiation of a further disturbance propagating downstream from the gate (in the Q plot), and finally a reflection of the gate disturbance from the upstream boundary (in the η plot). All this is as anticipated in Figure 9.3.

Figure 9.5 shows a detail in the neighborhood of the gate, and Figure 9.6 the water surface elevations η_B and η_C each side of the gate, and the corresponding flows Q_B and Q_C (which should be identical). Both are very clean. There is evidence of characteristic events 1,5 and 3 in Figure 9.3. But there is no evidence of any initial gate transients in either Figures 9.5 or 9.6, despite the sudden rise in water surface elevation at about 650 s on arrival of the characteristic Aa1 at point 1 (Figure 9.3). The visually smooth response and the specific absence of initial transients from either A or BC suggests heavy damping of shorter wave length responses.

The evidence from Figure 9.4 at A ($x = 0$) suggests that the CCW code heavily damps the shorter wave length modes that were expected (see §9.3) from the step change in Q at A. Heavy damping is in fact an implicit and documented² property of the three-point method of characteristics algorithm. While strong numerical filtering of the shorter response modes should not be a problem in many typical Bay-Delta applications, there are some applications (levee breaks, flow control structures, diversions, extreme floods, tsunami penetration, salinity barriers, ...) where this may be a concern.

The evidence from Figure 9.6 at BC ($x = 20,000$ ft) also suggest that the CCW code does include specific damping of gate transients. This is acknowledged³ by CCW. Their approach seems well researched and appropriate,

Figure 9.7 shows the time history of the mass and momentum balances at locations $x = 3,000$ ft and 23,000 ft. There are suggestions⁴ of initial transients here. In part (a) for $x = 3,000$ ft,

²In its primitive form, the three-point method of characteristics algorithm is equivalent (Hoffman 1992, p.747) to the Lax scheme. And the Lax scheme strongly damps the short wavelength modes (Abbott 1979, p.158 and Hoffman 1992, Figure 15.4).

³The following commentary was provided by CCW (Shum, 27 April 2001): “In most simulations, the alternating “overshoot” and “undershoot” of the predicted gate flow from the steady-state solution leads to the so-called wiggles. These “wiggles”, however, are numerical and not physical, and decreases in magnitude with smaller grid size and time step. In extreme cases when both the gate coefficient and time step are large whereas surface slope on the two sides are small, simulating gate flows using instantaneous stages at the two sides of the gate could lead to a reverse of the direction of the flow at the next time-step even though the water level away from the gate at the upstream end is higher than the downstream end.

Many numerical schemes use a weighted-average of the computed flows through the gate over two or more time-steps. ... An important consideration for simulating gate flows is to adjust this weighting-scheme to the time-step, the gate coefficient, and the hydraulic characteristics such as the surface slopes both upstream and downstream. There is no unique or best answer under all hydrological conditions in the Delta. The Fischer Delta Model uses a 0.75-0.25 (factors for the simulated flow in the previous and the current time-step, respectively) weighting-scheme to compute the flow through the gate at each time-step.

This weighting-scheme is based on empirical tests. These numerical characteristics need to be described in the report so that readers of the peer review can understand these considerations. The reference to ‘smooth is beautiful’ disease is inappropriate.”

⁴Sudden changes are not sufficiently gradually varied to be resolved by the numerical code, and a local imbalance in mass and/or momentum might be expected. But the local imbalances are not as strong as expected, presumably because of the strong numerical filtering of the shorter modes. At all other times, mass and momentum should be conserved.

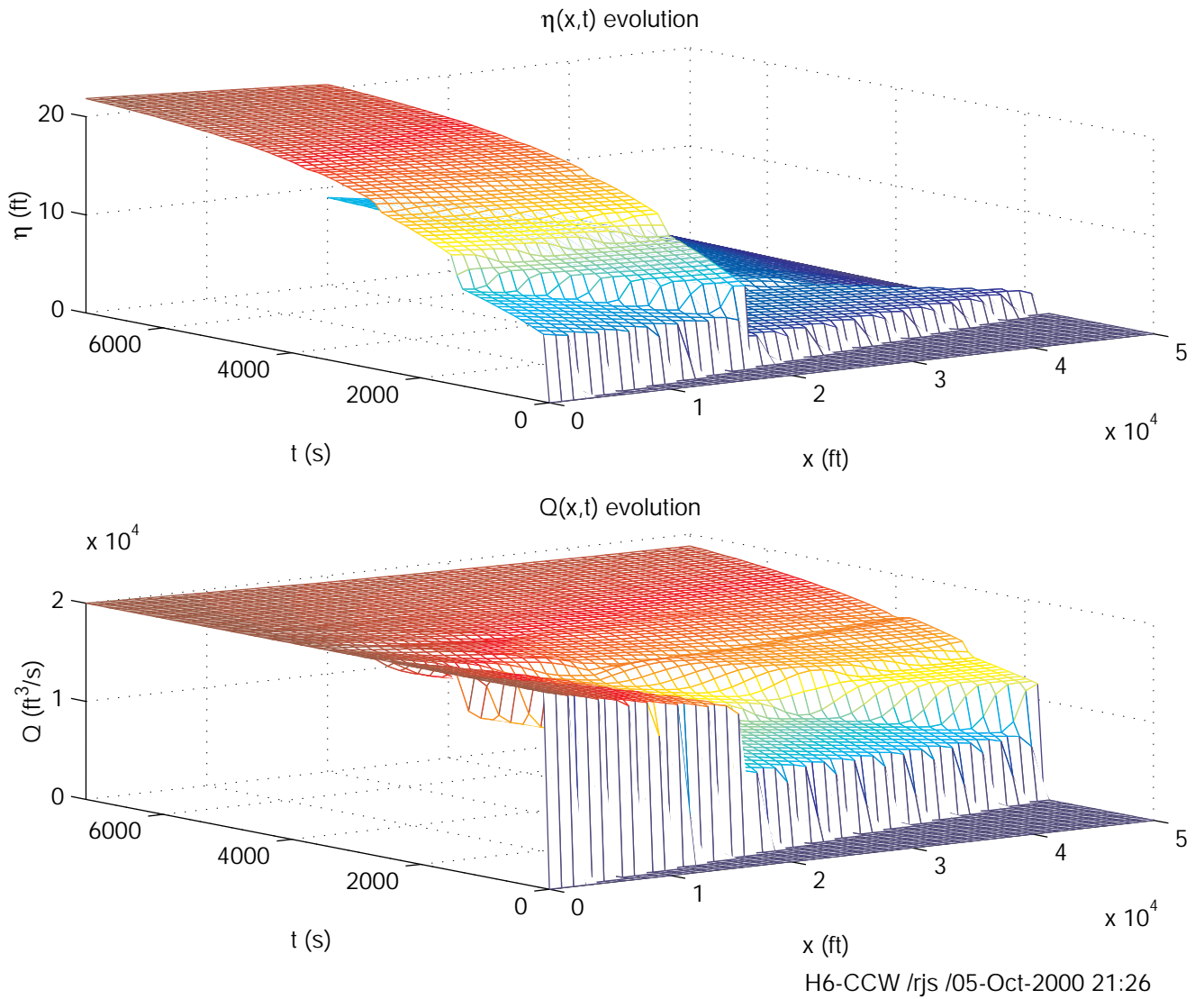
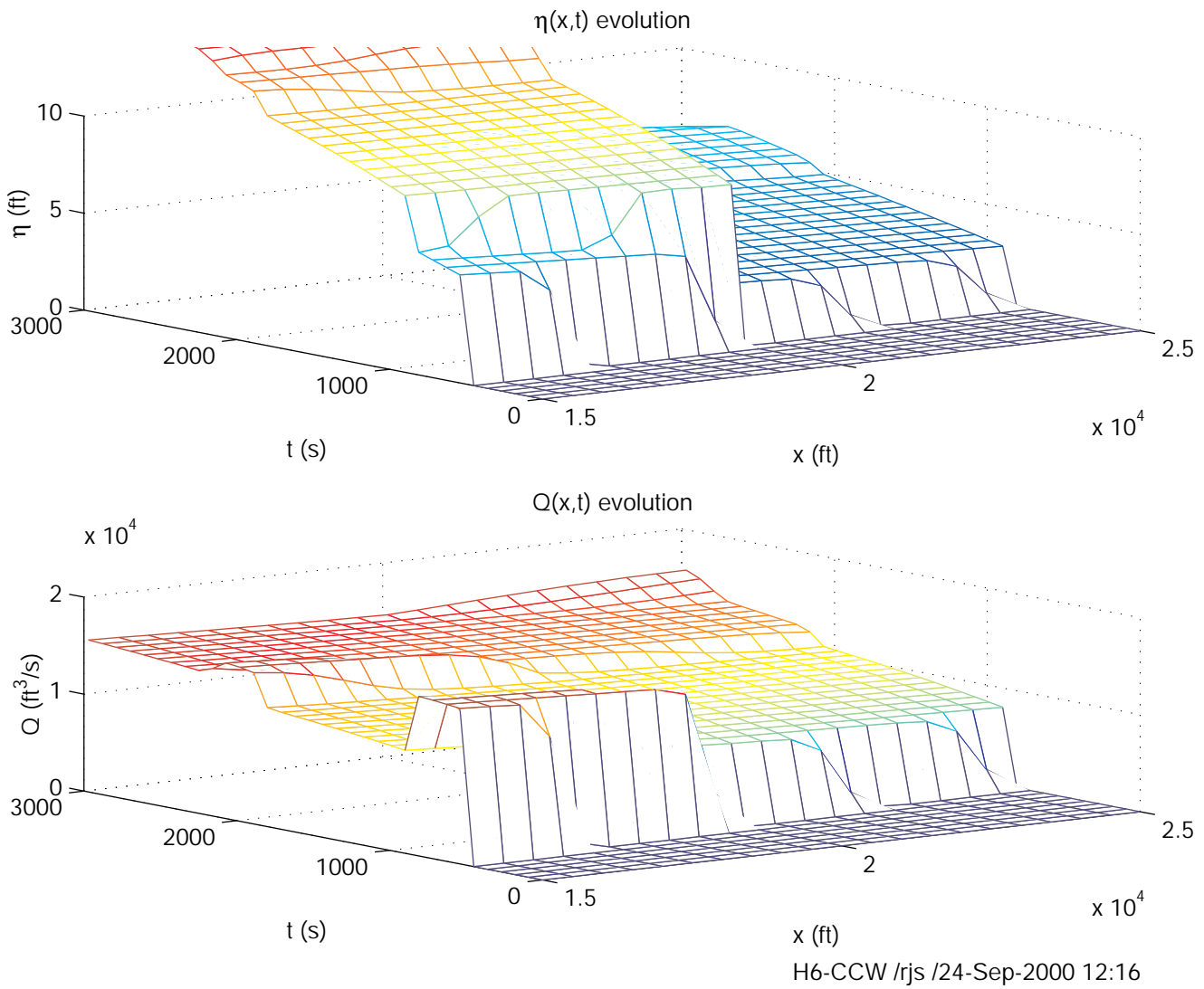
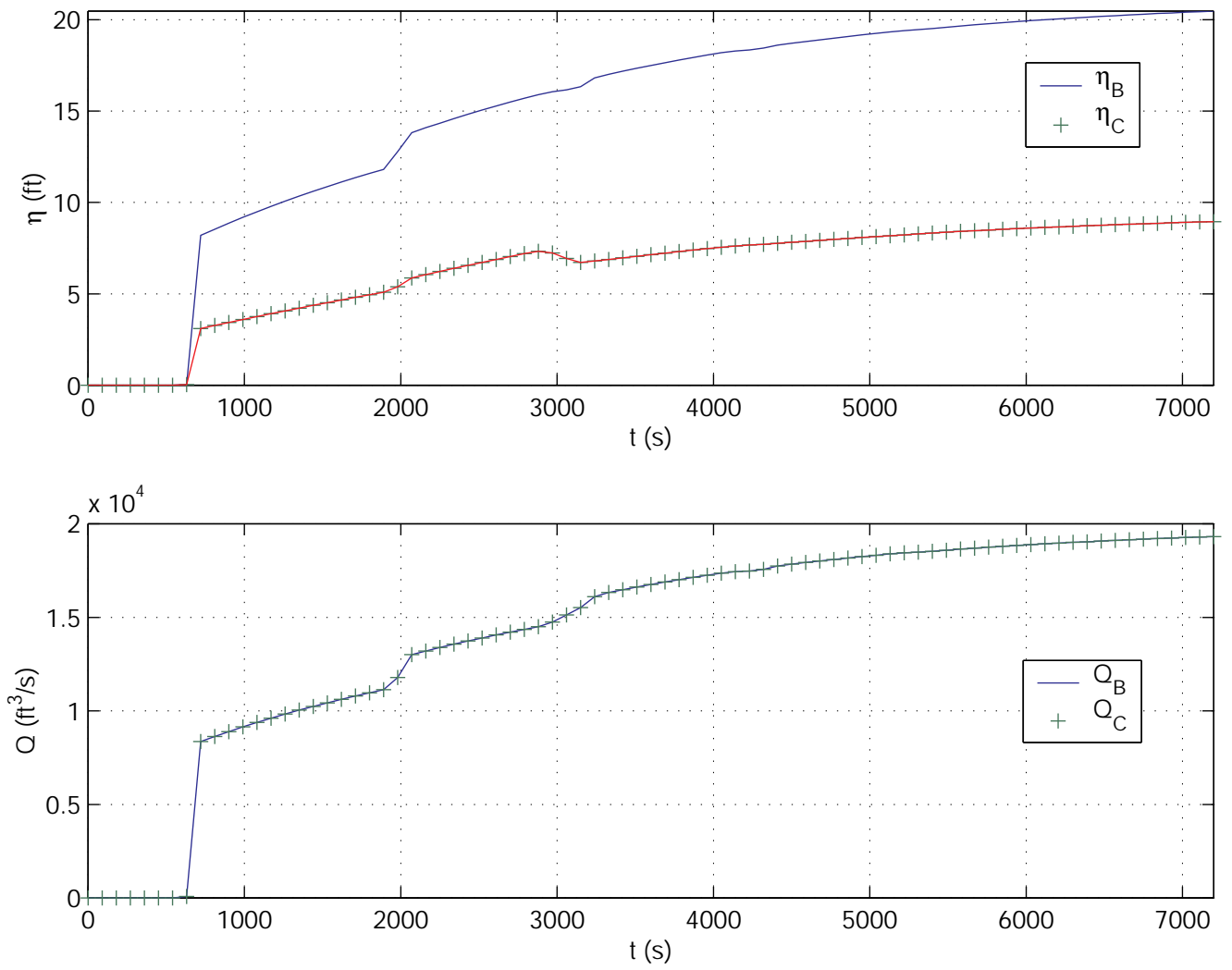


Figure 9.4: H6 CCW-predicted η and Q solution field evolution.



H6-CCW /rjs /24-Sep-2000 12:16

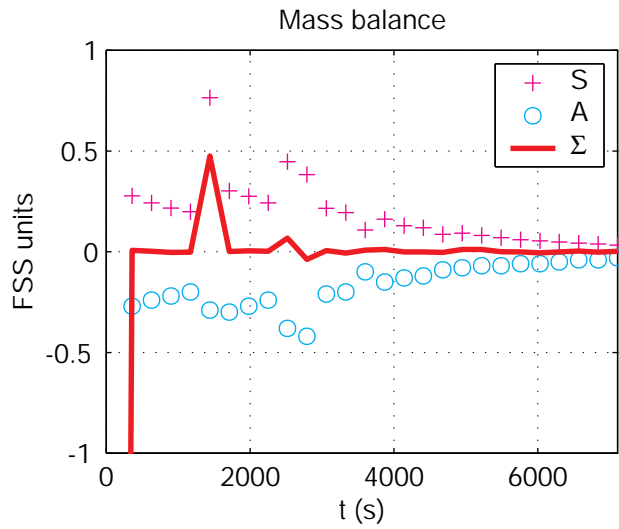
Figure 9.5: H6 CCW-predicted η and Q solution field evolution in neighborhood of gate.



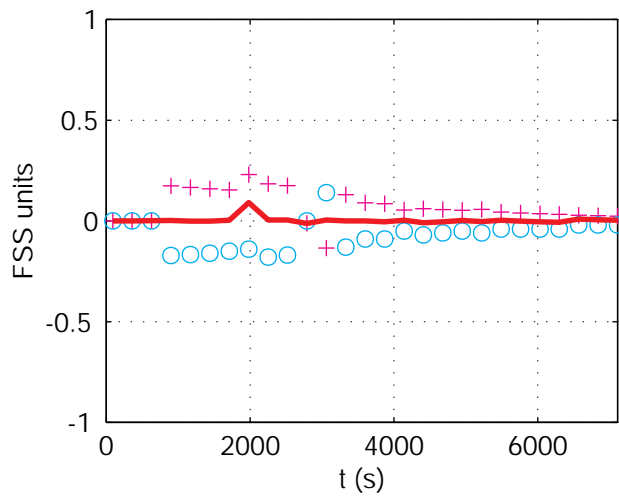
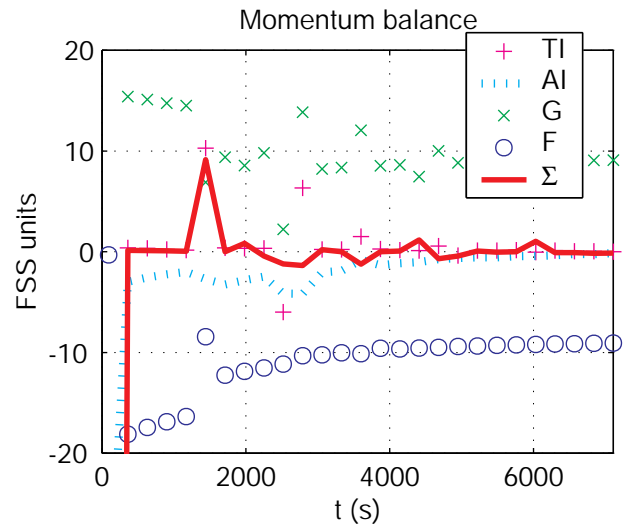
H6-CCW-Gate /rjs /28-May-2001 18:44

Figure 9.6: H6 CCW-predicted η and Q evolution at gate.

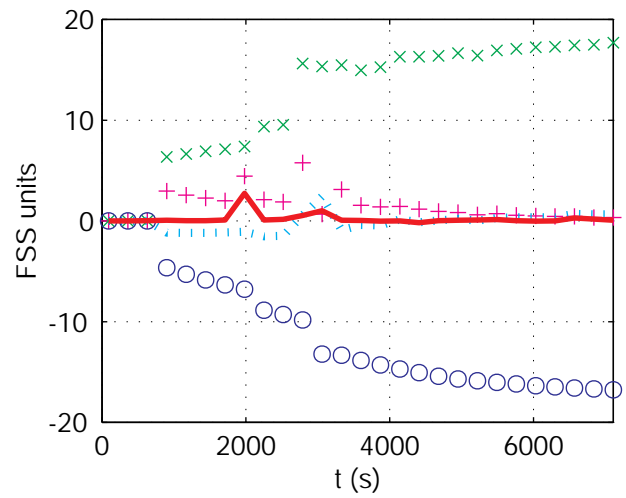
there is an out-of-balance spike in mass and/or momentum conservation at times corresponding to locations a, b and c in Figure 9.3. In part (b) for $x = 23,000$ ft, there are suggestions of transients at at times corresponding to d, e, and f in Figure 9.3. This is the expected response.



(a) $x = 3,000$ ft



(b) $x = 23,000$ ft



H6-CCW-55 /rjs /27-May-2001 20:02

Figure 9.7: H6 CCW-predicted conservation balances at $x = 3,000$ ft and $23,000$ ft.

9.5 Department of Water Resources

Figure 9.8 shows the DWR-predicted⁵ η and Q evolution toward the steady state. This is a visually impressive result. The characteristic paths are shown very clearly, in particular the initial disturbance propagating from the upstream boundary, the reflection of this disturbance from the gate (in the η plot) and from the downstream boundary (in the Q plot), the initiation of a further disturbance propagating downstream from the gate (in the Q plot), and finally a reflection of the gate disturbance from the upstream boundary (in the η plot).

There is a weak suggestion of initial transients from A in the Q response, Figure 9.8b. The absence of a strong but aliased initial transient response suggests that the DWR code heavily damps the shorter wave length modes that were expected (see §9.3) from the step change in Q at A. The likelihood of heavy numerical damping was anticipated in an earlier (see §3.2.2) discussion of the box algorithm adopted by DWR. While strong numerical filtering of the shorter response modes should not be a problem in many typical Bay-Delta applications, there are some applications (levee breaks, flow control structures, diversions, extreme floods, tsunami penetration, salinity barriers, ...) where this may be a concern.

Figure 9.9 shows a detail in the neighborhood of the gate, and Figure 9.10 the water surface elevations η_B and η_C each side of the gate, and the corresponding flows Q_B and Q_C (which should be identical). Both are very clean. There is evidence of characteristic events 1,5 and 3 in Figure 9.3. But there is no evidence of any free mode generation at the gate, despite the sudden rise in water surface elevation at about 650 s on arrival of the characteristic Aa1 at point 1 (Figure 9.3). The smooth $Q_B(t)$ (or $Q_C(t)$) evolution in the neighborhood of event 1, in particular, suggests that the DWR code does include⁶ specific damping of gate transients. It is possible that any gate transients are aggressively damped by the box algorithm's implicit numerical filtering of the shorter modes.

Figure 9.11 shows the time history of the mass and momentum balances at locations $x = 3,000$ ft and 23,000 ft. Mass and momentum are generally conserved at these selected locations upstream and downstream of the gate. The exceptions are a sequence of identifiable spikes that correspond with locations a, b and c in part (a) and d, e and f in part (b). This is the expected response.

⁵The DWR data file reports the output time step as 1 s; it was apparently not the specified 90 s, but 60 s. The output time step has been changed to 60 s for the following analyses.

⁶The following commentary was provided by DWR (2 February 2001): "This is not correct. DSM2 does not use filters of any kind. Based on our experience, DSM2 has always produced a smooth response in and around gates, except when extremely wide/deep weirs are simulated with large time steps ($\Delta t > 15$ minutes)."

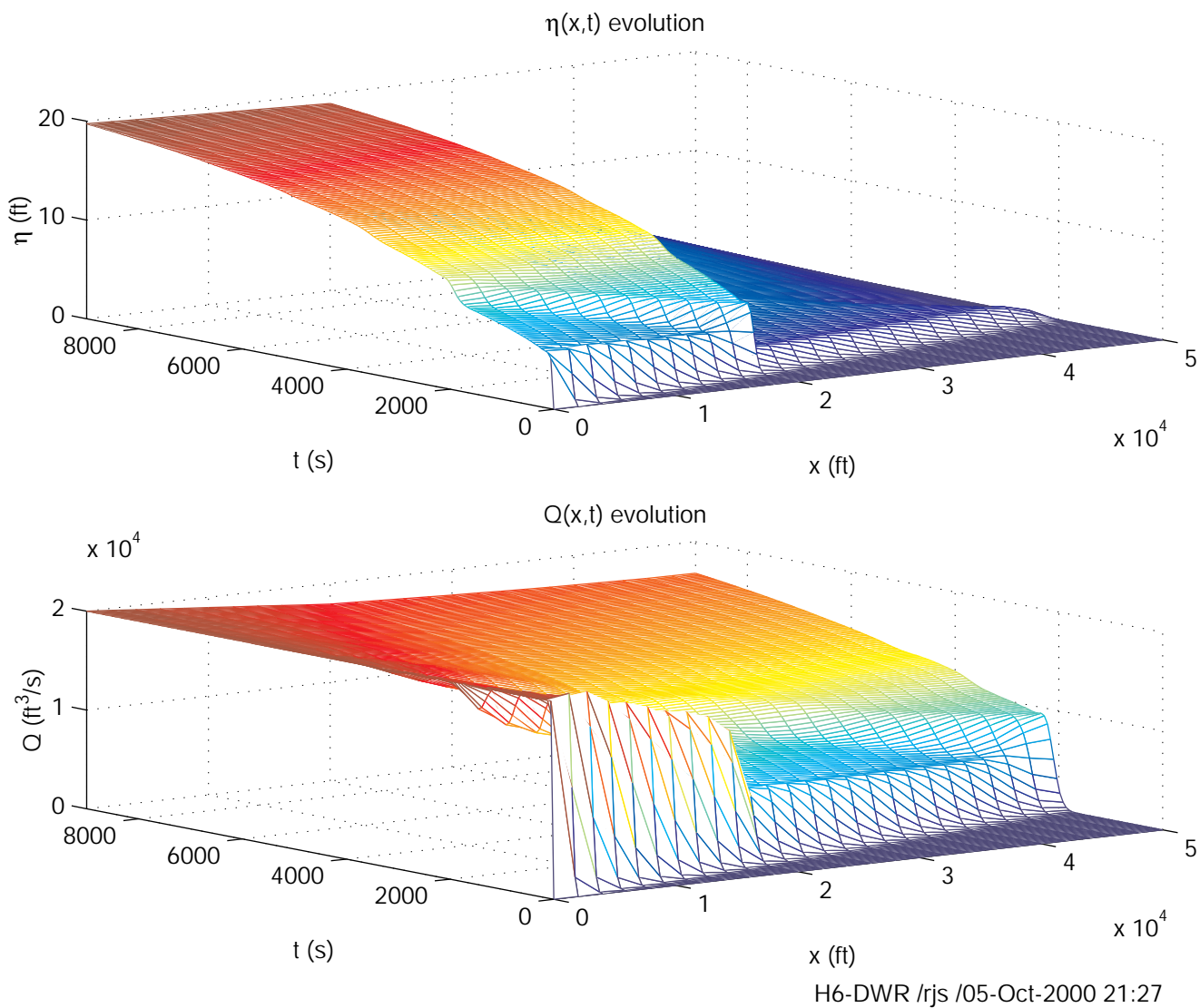
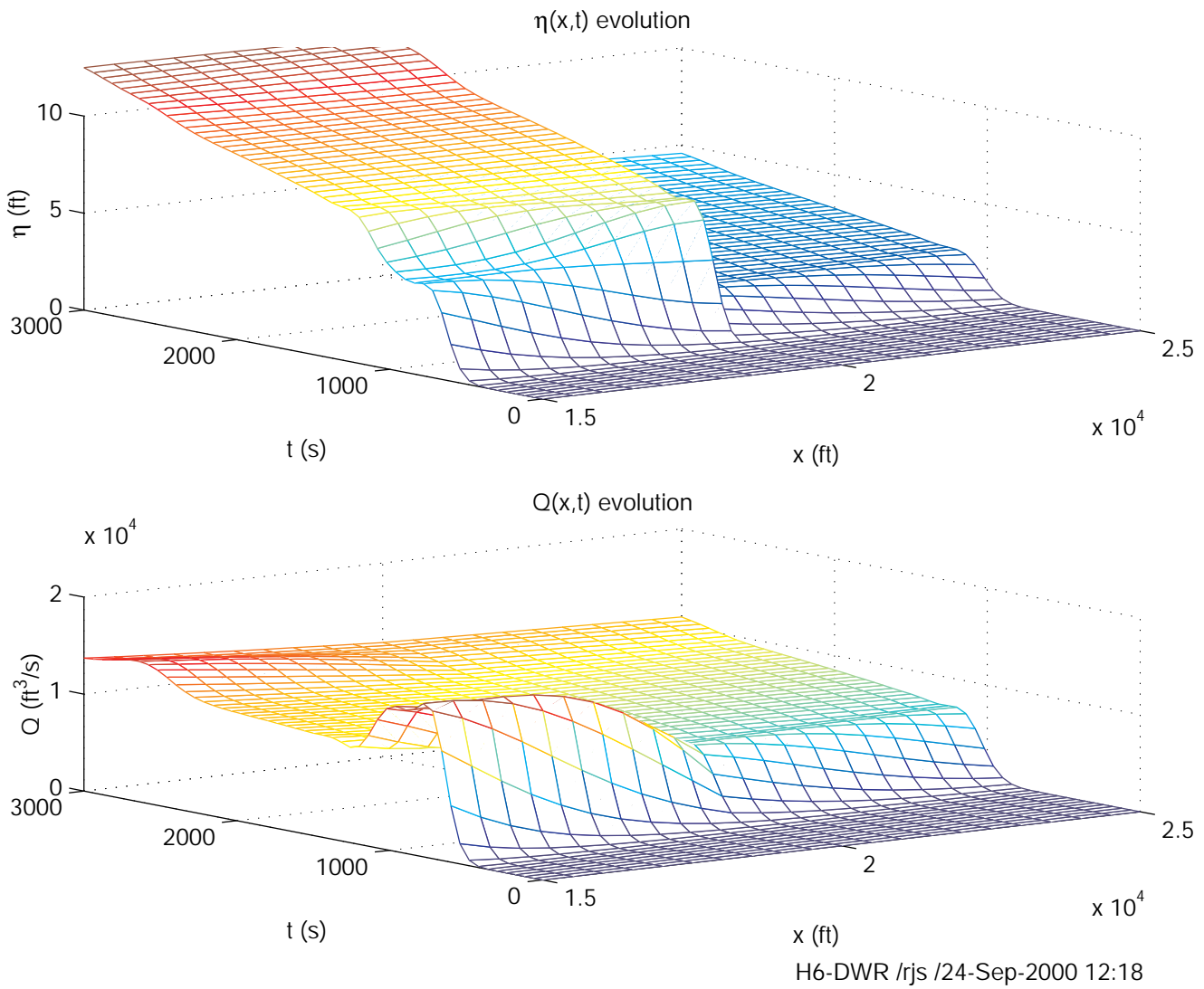
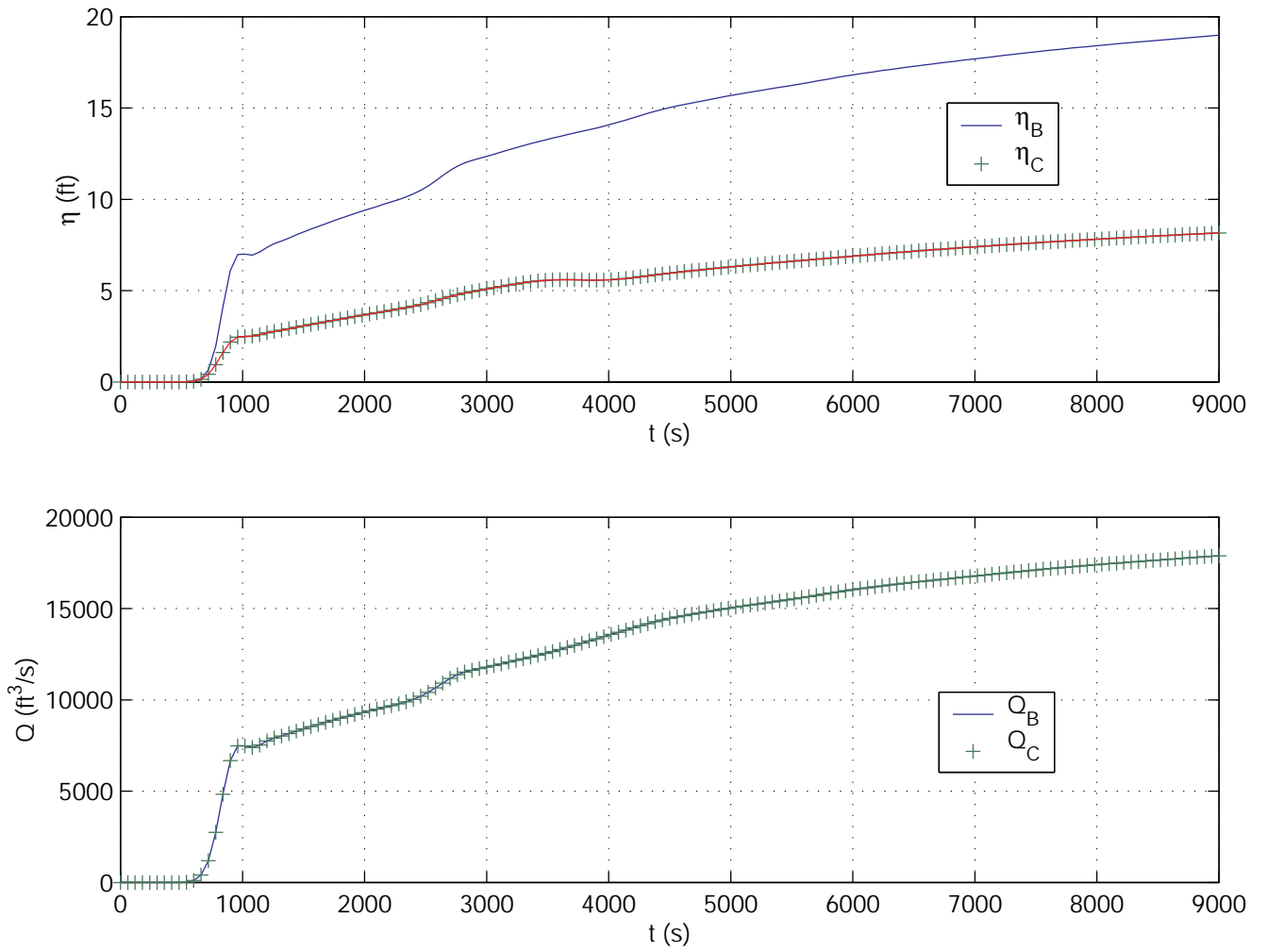


Figure 9.8: H6 DWR-predicted η and Q solution field evolution.



H6-DWR /rjs /24-Sep-2000 12:18

Figure 9.9: H6 DWR-predicted η and Q solution field evolution in neighborhood of gate.



H6-DWR-Gate /rjs /28-May-2001 18:45

Figure 9.10: H6 DWR-predicted η and Q evolution at gate.

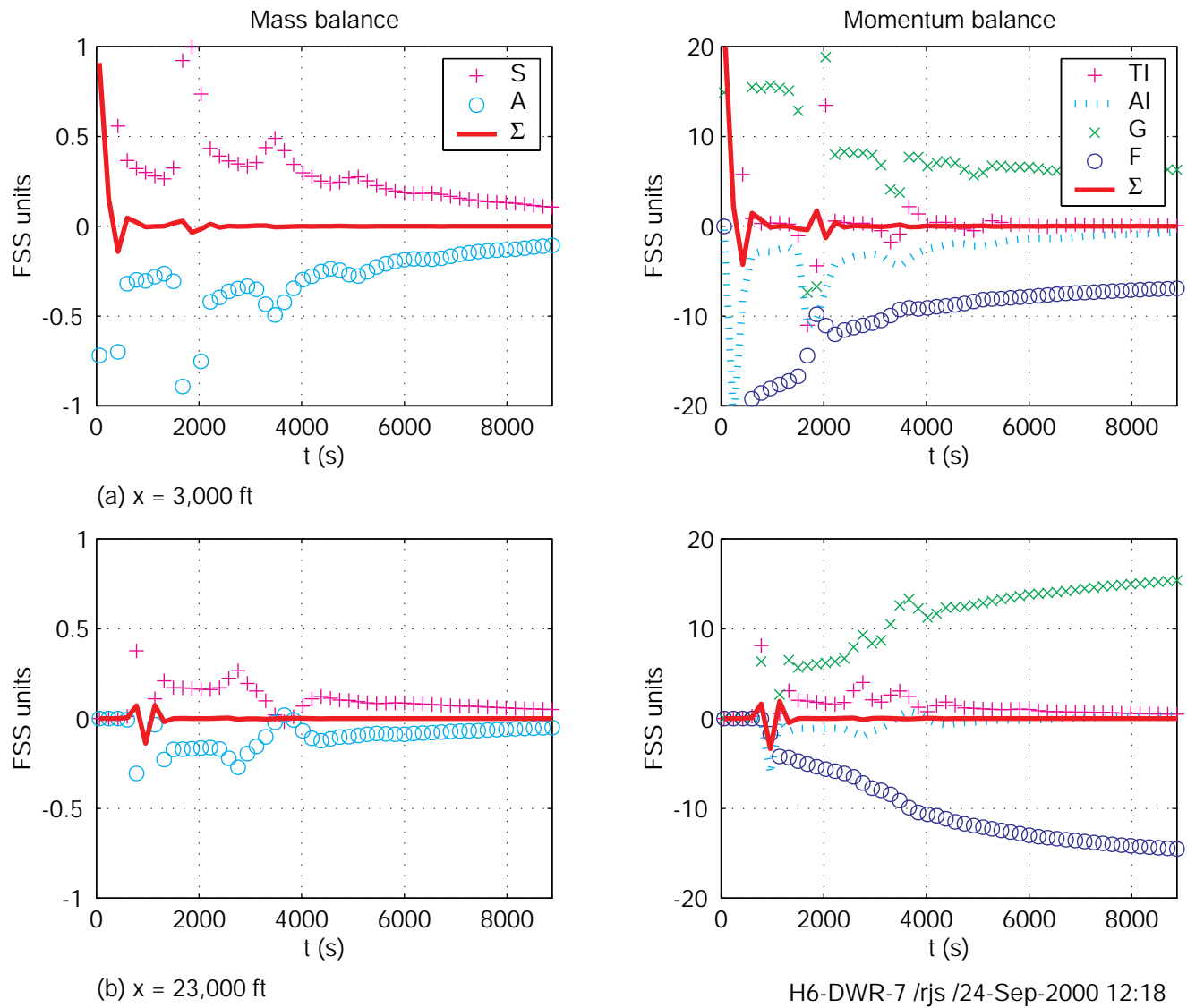


Figure 9.11: H6 DWR-predicted conservation balances at $x = 3,000$ ft and $23,000$ ft.

9.6 Resource Management Associates

Figure 9.12 shows the RMA-predicted⁷ η and Q evolution toward the steady state. As for the CCW and DWR results (Figures 9.4 and 9.8), this is a visually impressive result. The characteristic paths are shown very clearly, in particular the initial disturbance propagating from the upstream boundary, the reflection of this disturbance from the gate (in the η plot) and from the downstream boundary (in the Q plot), the initiation of a further disturbance propagating downstream from the gate (in the Q plot), and finally a reflection of the gate disturbance from the upstream boundary (in the η plot). All this is as anticipated in Figure 9.3.

Initial transients from the step change in Q at A are an evident feature. These transients (§3.2.2) are the expected response. There seems to be little numerical damping of the shorter wavelength modes by the RMA numerical algorithm, in contrast to the strong numerical damping with the CCW (Figure 9.4) and DWR (Figure 9.8) results. As expected, these disturbances are gradually decayed by friction. This is the expected result.

Figure 9.13 shows a detail in the neighborhood of the gate, and Figure 9.14 the water surface elevations η_B and η_C each side of the gate, and the corresponding flows Q_B and Q_C (which should be identical). There is evidence of characteristic events 1,5 and 3 in Figure 9.3. But there is no clear evidence of any free mode generation at the gate, despite the sudden rise in water surface elevation at about 650 s on arrival of the characteristic Aa1 at point 1 (Figure 9.3). The moderately smooth $Q_B(t)$ (or $Q_C(t)$) evolution in the neighborhood of event 1 perhaps suggests that the RMA code does include specific damping of gate transients. It is possible that any gate transients are aggressively damped by the box algorithm's implicit numerical filtering of the shorter modes.

Figure 9.15 shows the time history of the mass and momentum balances at locations $x = 3,000$ ft and 23,000 ft. Mass and momentum are generally conserved at these selected locations upstream and downstream of the gate. The exceptions are a sequence of identifiable spikes that correspond with locations a, b and c in part (a) and d, e and f in part (b). The c and d spikes are especially strong, but this is consistent with non-suppression of the shorter wavelengths. This is the expected response.

REFERENCES

- Abbott, M. B. (1979). *Computational Hydraulics*. Pitman, London.
- Båth, M. (1974). *Spectral Analysis in Geophysics*. Elsevier, Amsterdam.
- Bode, L. and R. J. Sobey (1984). Initial transients in long wave computations. *Journal of Hydraulic Engineering* 110, 1371–1397.
- Gresho, P. M. and R. L. Lee (1981). Don't suppress the wiggles - they're telling you something! *Computers and Fluids* 9, 223–253.
- Hoffman, J. D. (1992). *Numerical Methods for Engineers and Scientists*. McGraw-Hill, New York.

⁷The RMA predictions have used a space step Δx of 250 ft, not the required 500 ft.

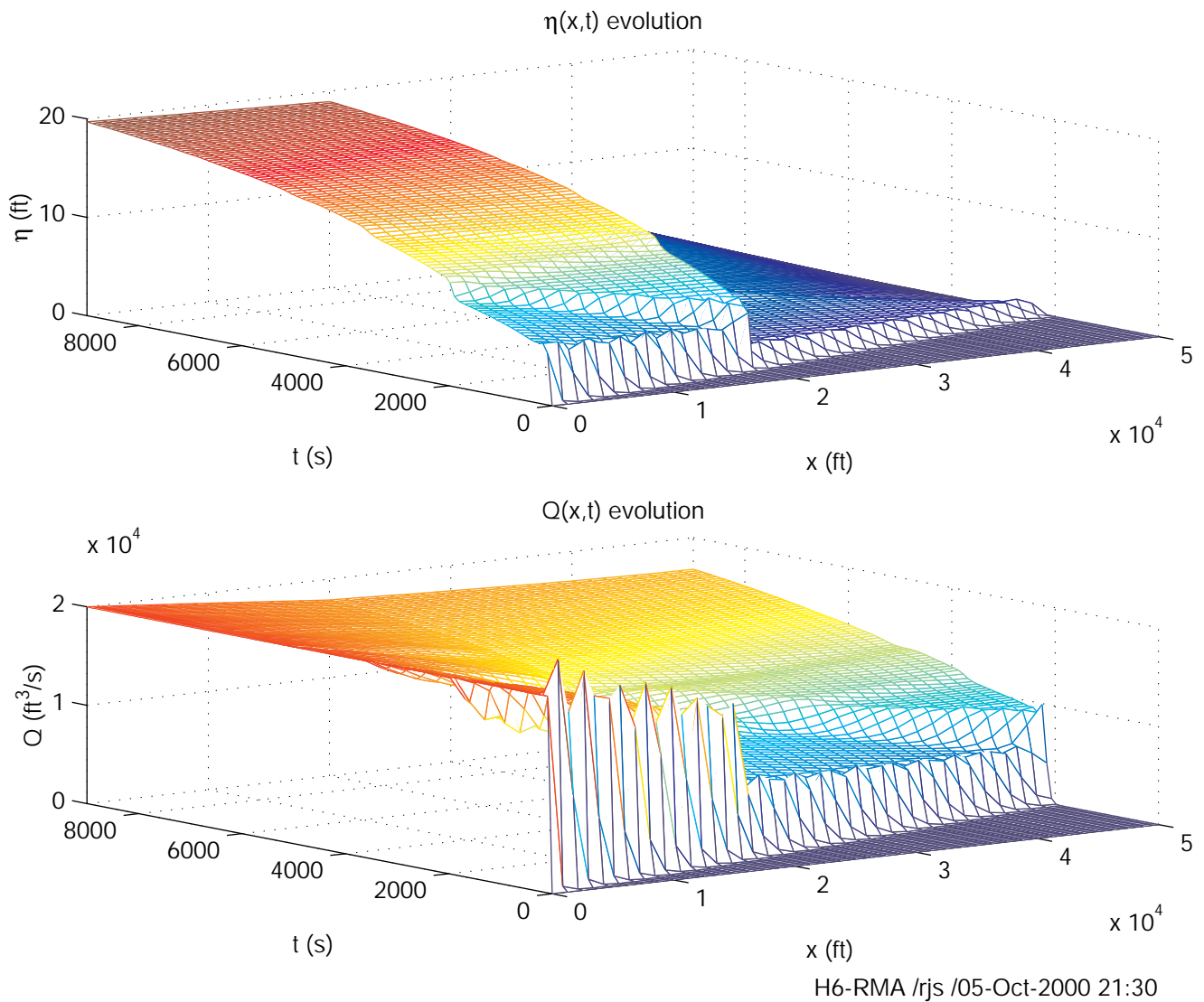
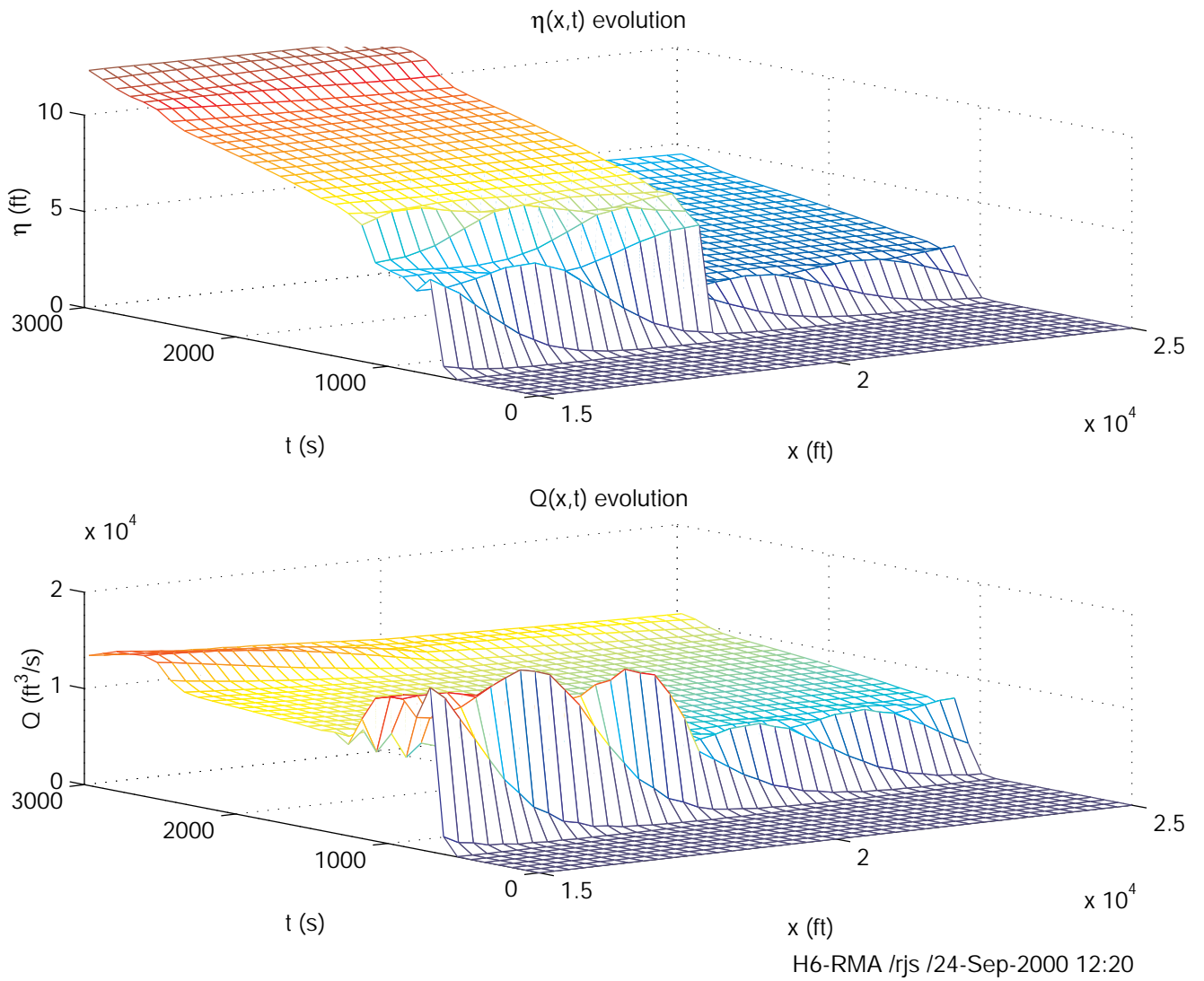
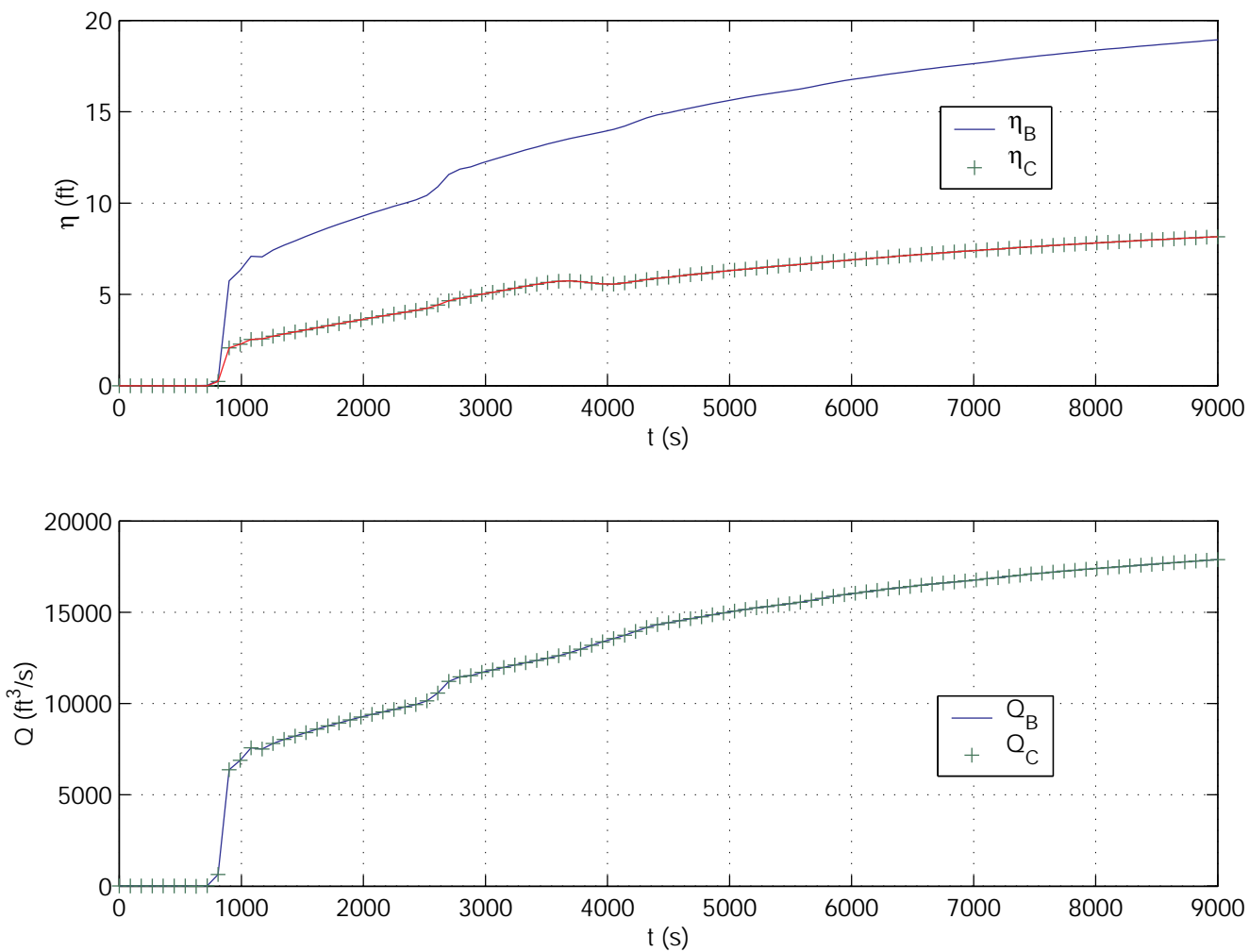


Figure 9.12: H6 RMA-predicted η and Q solution field evolution.



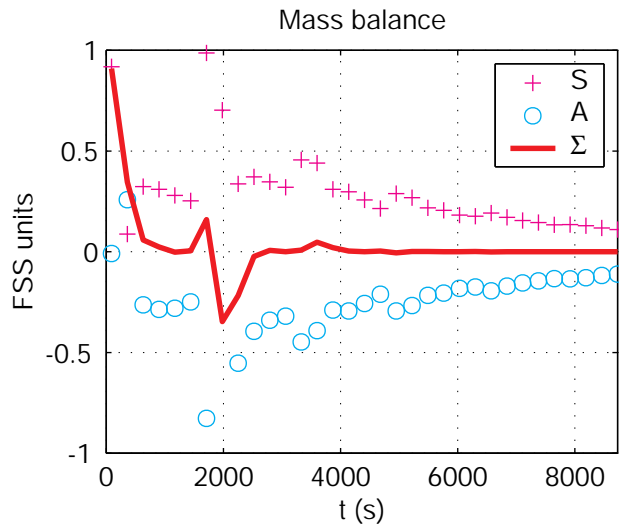
H6-RMA /rjs /24-Sep-2000 12:20

Figure 9.13: H6 RMA-predicted η and Q solution field evolution in neighborhood of gate.

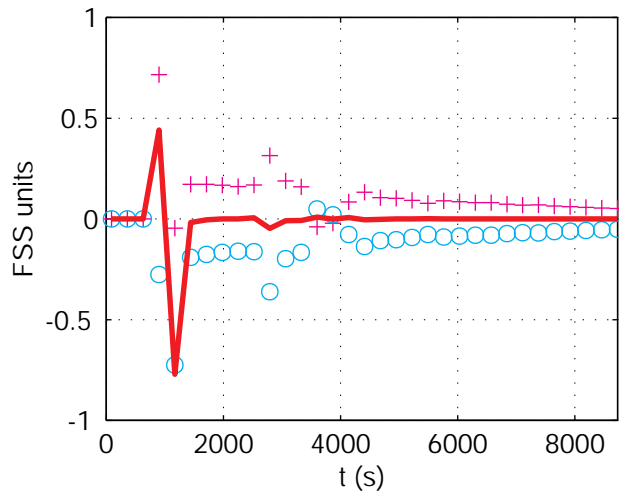
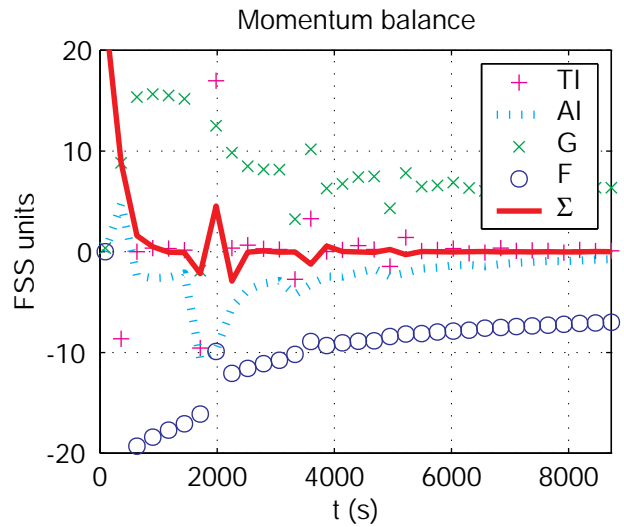


H6-RMA-Gate /rjs /28-May-2001 18:47

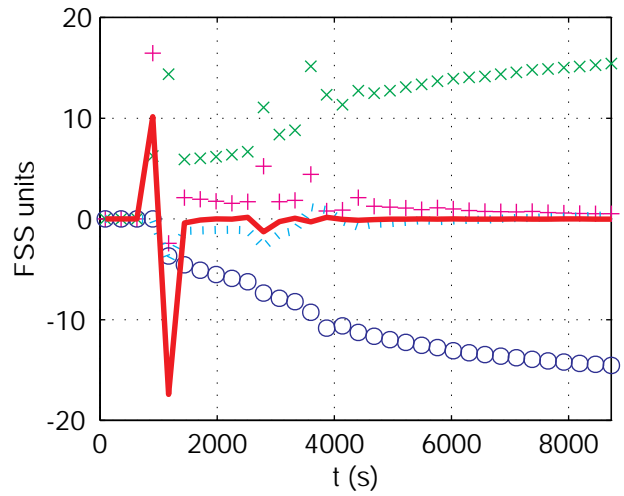
Figure 9.14: H6 RMA-predicted η and Q evolution at gate.



(a) $x = 3,000$ ft



(b) $x = 23,000$ ft



H6-RMA-13 /rjs /24-Sep-2000 12:20

Figure 9.15: H6 RMA-predicted conservation balances at $x = 3,000$ ft and $23,000$ ft.